VIP Nanotube Self-Assembly

DOI: 10.1002/anie.201003415

Amphiphilic Self-Assembly of an n-Type Nanotube**

*Hui Shao, James Seifert, Natalie C. Romano, Min Gao, Jonathan J. Helmus, Christopher P. Jaroniec, David A. Modarelli, and Jon R. Parquette**

The electronic properties of π-conjugated materials depend on the nature of the interactions among the constituent chromophores.[1] The π–π stacking interactions present in aggregated arrays of semiconductors provide pathways for charge transport and energy migration.[2] Thus, the self-assembly of π-conjugated building blocks into discrete, one-dimensional (1D) nanostructures is a powerful strategy to tune the properties of organic electronic materials.[3] The majority of these approaches have produced twisted nanofibers of p-type chromophores. The exceptional electronic characteristics of carbon nanotubes[4] have also inspired interest in versatile supramolecular approaches toward π-conjugated nanotubes.[5] The availability of self-assembled organic nanotubes would provide greater modularity in their design and functionalization. However, examples of π-conjugated systems that assemble into well-defined nanotubes are relatively uncommon.[6] Herein, we describe a 1D n-type nanotube formed by the bolaamphiphilic[7] self-assembly of 1,4,5,8-naphthalenetetracarboxylic acid diimide (NDI) with L-lysine headgroups (Figure 1).

We recently reported a simple method for fabricating n-type 1D nanostructures by the β-sheet assembly of dipeptide–NDI conjugates[8] into either helical nanofibers or twisted nanoribbons.[9] Time-resolved fluorescence anisotropy experiments showed enhanced energy migration within these nanostructures. Herein, we explore how the intermolecular electrostatic interactions derived from the lysine headgroups[10] in bolaamphiphile **A** (Figure 1a), in conjunction with π–π association among the NDI chromophores, drive the self-assembly process in water[11,12] toward soluble, well-ordered 1D nanotubes.

Bolaamphiphile **A** was constructed by imidation of 1,4,5,8-naphthalenetetracarboxylic acid dianhydride with two equivalents of Boc-L-lysine, followed by TFA deprotection (Supporting Information, Scheme S1). Bolaamphiphile **A** formed a transparent gel in water at concentrations as low as 1% (w/w) (1.9 mM; Figure 1b, red inset), and was stable in the gel state for several months. Transmission electron microscopy (TEM) of a negatively stained sample of **A** revealed the formation of micrometer-long nanotubes with uniform diameters of (12 ± 1) nm (Figure 1b). The nanotubes appeared as two white, parallel lines separated by a dark center, which is consistent with the cross-sectional view of a hollow tubular structure filled with the negative stain, uranyl acetate (Figure 1b).[13] The thickness of the wall was approximately (2.5 ± 0.5) nm. A few nanorings, albeit rare, could also be observed in the TEM images (red arrows in Figure 1b), with external diameters of 12 nm and wall thicknesses of 2.5 nm, which are identical with the nanotube dimensions. Tapping-mode AFM imaging of dilute bolaamphiphile **A** gel samples (250 μM) on mica also revealed high-aspect ratio assemblies with cross-sectional heights of about 9 nm, which were slightly smaller than those observed by TEM; this effect

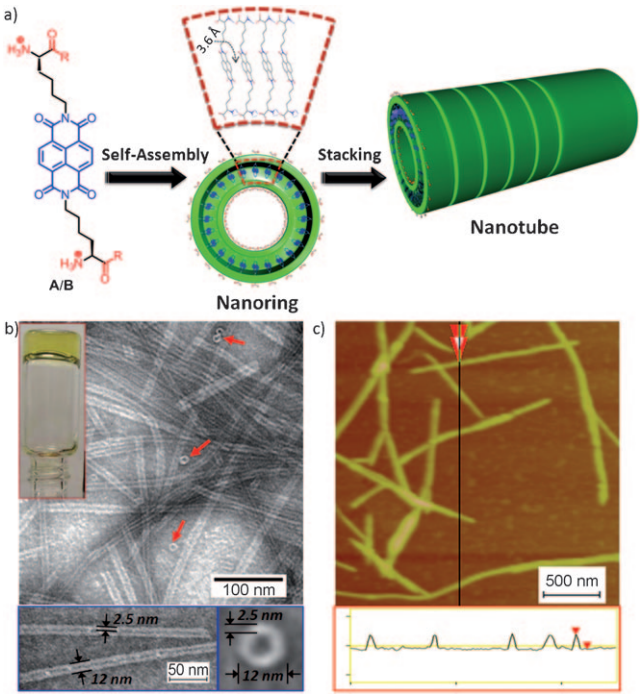

Figure 1. a) Structures of lysine-based bolaamphiphiles **A** (R = O^-) and **B** (R = OMe) and the assembly of **A** into rings, which stack to give tubes. The blue sections of **A** undergo hydrophobic π–π stacking interactions, and the red sections electrostatic interactions. b) TEM image of bolaamphiphile **A** in water (250 μM; carbon-coated copper grid); 2% (w/w) uranyl acetate as negative stain. Blue insets: Two nanotubes and one nanoring. c) Tapping-mode AFM image of bolaamphiphile **A** in water (250 μM) on freshly cleaved mica. Red inset: Section analysis showing uniform height of the assemblies. Height indicated by red arrows: ca. 9 nm.

[*] H. Shao, J. Seifert, M. Gao, J. J. Helmus, Prof. C. P. Jaroniec, Prof. J. R. Parquette
Department of Chemistry, The Ohio State University
100 W. 18th Ave., Columbus, OH 43210 (USA)
E-mail: parquett@chemistry.ohio-state.edu
N. C. Romano, Prof. D. A. Modarelli
Department of Chemistry and
The Center for Laser and Optical Spectroscopy
The University of Akron (USA)

[**] This work was supported by the National Science Foundation (CHE-0750004 and CRC-CHE-526864).

Supporting information for this article is available on the WWW under http://dx.doi.org/10.1002/anie.201003415.

is most likely due to the compression of the nanotube by the AFM tip. A condensed entangled nanotube network was observed upon forming the gel at higher concentration of **A** (Supporting Information, Figure S2). In contrast, no ordered structures could be observed by TEM or AFM in 2,2,2-trifluoroethanol (TFE). The corresponding methyl ester **B** did not form a gel (in water or TFE) or exhibit any observable nanostructures by TEM (Supporting Information, Figure S2), presumably because of the inability to engage in attractive electrostatic interactions.[14]

Evidence for π–π stacking of NDI chromophores within the nanostructure of bolaamphiphile **A** in water was apparent in UV spectra. A decrease in the absorption intensities (54% in Band I (300–400 nm) and 20% in Band II (236 nm)), along with band broadening, accompanied nanotube formation in water (Figure 2a). Furthermore, red-shifts of 8 nm (Band I) and 10 nm (Band II), which occurred going from TFE to water, are consistent with the presence of *J*-type π–π stacking

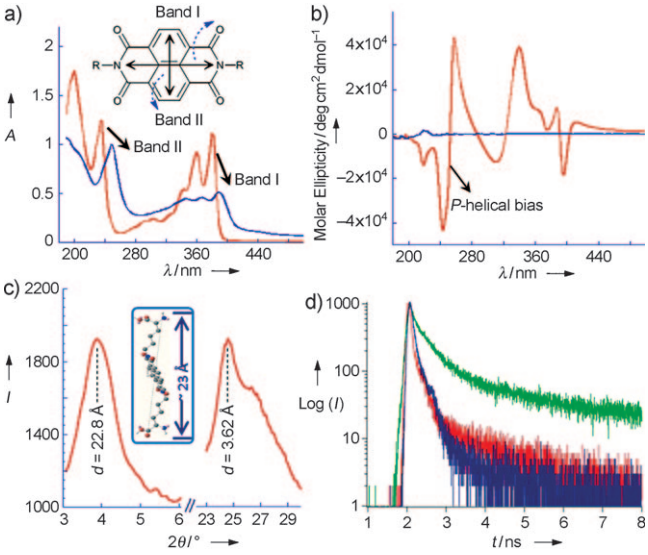

Figure 2. a) UV spectra of bolaamphiphile **A** in TFE (red) and water (blue; 500 μM). Inset: Principal *z*-polarized and *y*-polarized π→π* transitions in NDI chromophore: Band I (*z*, 300–400 nm), Band II (*y*, 200–260 nm). b) CD spectra of bolaamphiphiles **A** (red) and **B** (blue) in water (250 μM). c) XRD pattern of the gel formed by bolaamphiphile **A**. d) Time-resolved fluorescence spectra of **A** and **B** in water. Red: bola A at 410 nm; green: bola A at 505 nm; blue: bola B at 410 nm.

of the NDI chromophores.[15] The UV spectra of **B** were quite similar in TFE and water (Supporting Information, Figure S3), which is consistent with the molecularly dissolved state of **B** in both solvents. The long-range orientation of NDIs within the assembled nanotubes was investigated by comparing the circular dichroism (CD) spectra of bolaamphiphiles **A** and **B** in H_2O (Figure 2b). Whereas the CD spectrum of **B** displayed a flat profile in water, **A** exhibited strong positive excitonic couplets around the regions corresponding to both π→π* absorption bands I and II. The positive couplet centered at 248 nm indicates that the *y*-polarized transition dipoles of **A** (Figure 2a, inset) within the nanotubes are oriented in a right-handed, P-type helical arrangement.[16]

The XRD pattern for bolaamphiphile **A** prepared from the hydrogel showed a sharp reflection with a *d* spacing of 2.28 nm in the small-angle region (Figure 2c). This spacing correlates with the calculated length of fully extended **A** (2.3 nm) and the wall thickness of the nanotube (2.5 nm), as measured by TEM. The peak appearing at $d = 3.6$ Å in the XRD pattern corresponds to the π–π stacking distance between the NDI moieties in the nanotube, similar to the interplanar distances present in the crystal structure of NDI.[17]

A model for the self-assembly of bolaamphiphile **A** nanotubes is shown in Figure 1a. The occasional nanorings that are observed in the TEM images exhibit wall thicknesses and diameters that are nearly identical to those of the fully formed nanotubes. Furthermore, the extended length of **A** is similar to both the nanotube wall thickness and the XRD reflection at $d = 2.28$ nm. This result could be rationalized by the presence of a stable monolayer lipid membrane (MLM) within the assembly, which is commonly observed for bolaamphiphiles.[18,11] Thus, the nanotubes may initially assemble into a MLM that curves into the observed nanorings. The curvature of the MLM may emerge from the chirality of the headgroups, which induces the molecules to pack in tilted orientations.[19] The large hydrophobic/hydrophilic ratio may also enforce membrane curvature to reduce the surface edges exposed to water.[20] Subsequent stacking of the rings into the nanotube structure sequesters the hydrophobic NDI cores within the interior of the MLM tube wall while projecting the hydrophilic lysine headgroups on the inner and outer surfaces of nanotube.[21]

Nanotubes, prepared from natural-abundance bolaamphiphile **A**, and from **A** containing uniformly ^{13}C,^{15}N-enriched lysine headgroups, were further investigated by magic-angle spinning (MAS) solid-state NMR spectroscopy. 1D cross-polarization (CP) MAS NMR spectra obtained for ^{13}C,^{15}N-labeled nanotubes (Figure 3a) reveal two distinct signals for each lysine ^{13}C and ^{15}N site. Complete assignments (Supporting Information, Table S1) were obtained using 2D ^{13}C–^{13}C (Figure 3b) and ^{15}N–^{13}C (Figure 3c) chemical shift correlation spectra recorded using dipolar-assisted rotational resonance (DARR)[22] and transferred-echo double resonance (TEDOR),[23] respectively (resonances are identified according to the standard convention for lysine backbone and side-chain atoms, with a K1 or K2 prefix to denote lysines 1 and 2, respectively, as discussed in detail below). The ^{15}N resonance widths were found to be about 25 Hz (ca. 0.5 ppm at 500 MHz ^1H frequency), and the average widths of the K1 and K2 ^{13}C signals for natural abundance nanotubes (spectrum not shown) were (0.40 ± 0.04) and (0.7 ± 0.3) ppm, respectively (somewhat broader ^{13}C signals (ca. 0.8–1 ppm) were observed for the ^{13}C,^{15}N-labeled nanotubes, which is consistent with the additional contribution of ^{13}C–^{13}C *J* couplings to the linewidth). Such narrow linewidths are comparable to those typically observed for nanocrystalline peptides,[23] and are indicative of a relatively high degree of molecular ordering of bolaamphiphile **A** monomers within the nanotube scaffold. We also note that virtually superimposable ^{13}C spectra were

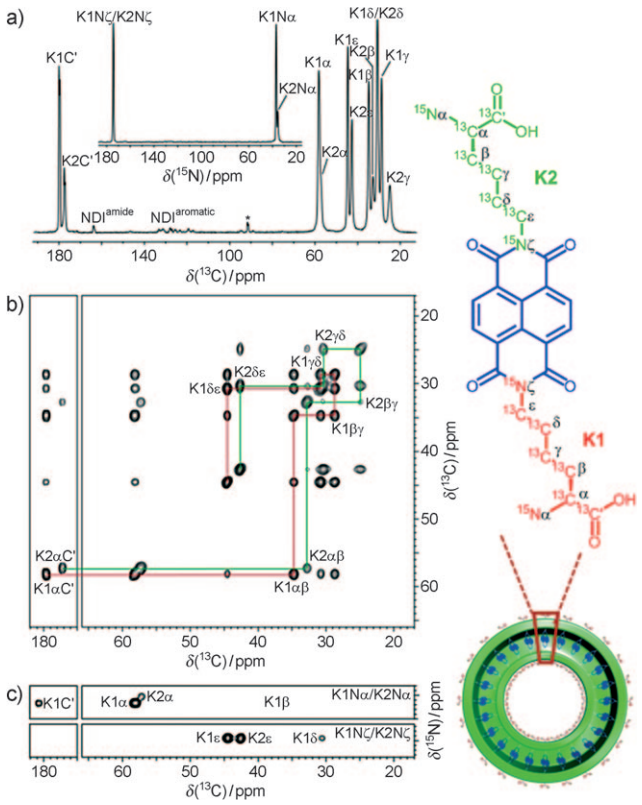

Figure 3. a) 1D ^{13}C and ^{15}N CP-MAS NMR spectra of ^{13}C,^{15}N-bolaamphiphile **A** nanotubes (1024 scans). Assignments are indicated; the asterisk denotes a spinning sideband. b) Small regions from DARR[22] ($t_{mix}=25$ ms) 2D ^{13}C–^{13}C correlation spectra, recorded with 16 scans per row, $t_{1,max}=12.2$ ms, $t_{2,max}=28$ ms, and a total experiment time of about 10 h. c) Strips from TEDOR[23] ($t_{mix}=2.16$ ms) 2D ^{15}N–^{13}C correlation spectra, corresponding to lysine $N\alpha$ and $N\zeta$ signals as indicated, recorded with 48 scans per row, $t_{1,max}=17.3$ ms, $t_{2,max}=25$ ms, and total experiment time of about 7 h. All of the NMR data were collected at 11.7 T, 11.111 kHz MAS rate, and a temperature of 0 °C.

obtained for the ^{13}C,^{15}N-labeled nanotubes and several independently prepared unlabeled nanotube samples, indicating high reproducibility of the experiments.

Although corresponding pairs of K1 and K2 resonances (that is, K1α and K2α, and so on) do not display equal integrated intensities in ^{13}C CP-MAS spectra (Figure 3a), they do so in fully relaxed, quantitative ^{13}C Bloch decay (one-pulse) spectra (Supporting Information, Figure S7). This implies that K1 and K2 subsets of signals correspond to the two lysine headgroups linked to the same central NDI moiety, one located on the inside and one on the outside of the nanotube. The most likely rationale for different resonance intensities of the two lysine headgroups relates to different conformational dynamics for bolaamphiphile **A** molecules within the nanotube hydrogels, and similar effects have been previously observed in CP-MAS spectra of fully-hydrated supramolecular amyloid aggregates composed of large protein molecules.[24] To further probe this issue, we have recorded a set of ^{13}C Bloch decay spectra as a function of temperature between −20 °C and 20 °C (Supporting Information, Figure S7). These data show that while the integrated intensities of K2 signals remain constant, as expected, the resonance widths vary significantly as a function of temperature, becoming narrower at higher temperatures and broader at lower temperatures. In contrast, the linewidths of the K1 signals are relatively insensitive to temperature. These observations are consistent with the presence of molecular motions on different timescales for the K1 and K2 headgroups. Based on these data and the assumption that the degree of molecular flexibility can be directly correlated with the amount of available conformational space, which would be greater on the outer surface of the nanotube, we hypothesize that the K1 and K2 subsets of signals correspond to the lysine headgroups located on the inner and outer surfaces of the nanotube, respectively (see model in Figure 3).

The fluorescence spectrum of **B** in water is typical of *N*,*N*-dialkyl-substituted NDIs, with a fluorescence band at 415 nm and a significantly less intense peak at 500 nm (Supporting Information, Figure S4).[25] In contrast, the fluorescence spectrum of **A** in water shows significant enhancement of the emission band at $\lambda_{em}\approx 505$ nm, whereas the peak at 415 nm becomes much less intense, which is consistent with inter-NDI electronic communication in the excited state between closely spaced, and spatially constrained, NDI groups. Time-correlated single photon counting (TCSPC) experiments with picosecond excitation at 350 nm were performed on **A** and **B** while following the emission decays of both compounds at 410 and 505 nm (Figure 2d). The experiments using 410 nm detection (λ_{410}) yielded short-lived decays ($\tau_{410}\approx 64$ ps) for both **A** and **B** that are slightly longer-lived than the singlet excited state lifetime of the parent *N*,*N*-di-*n*-butyl NDI ($\tau_{Fl}\approx 16.4$ ps, $\Phi_{Fl}\approx 0.002$).[25] Measuring the emission of **A** at 505 nm, however, revealed a significantly longer-lived biexponential decay with lifetime components of $\tau_{505,1}\approx 197$ ps (86%) and $\tau_{505,2}\approx 950$ ps (14%). A similar experiment for **B** was not successful because of the weak fluorescence signal at 505 nm. The long-lived fluorescence decay observed for **A** cannot result from dimers or oligomers formed within the short lifetime of the NDI excited state, and is therefore attributed to pre-association in the assemblies.

To further probe the excited state dynamics of **A**, time-resolved fluorescence anisotropy (TRFA) experiments were performed at 410 and 505 nm. In the TRFA experiments, rotational depolarization of the fluorescence signal is expected only for monomeric NDIs and not the self-assembled aggregates/nanotubes. In the latter, rapid depolarization resulting in low initial anisotropy (r_0) values has been shown to result from ultrafast energy transfer.[9a] As expected, the anisotropy data for the monomeric fluorescence band of **A** (λ_{em} 410 nm) exhibited a large initial anisotropy (r_0) of 0.38. However, the anisotropy decays of **A** at 505 nm yielded a r_0 value of $r_0(505\text{ nm})\approx 0.086$, which is consistent with rapid depolarization by energy transfer within assemblies. TRFA experiments on **B** were not possible because of the low fluorescence signal at either 410 or 505 nm. It is not known at this point whether energy transfer occurs along the nanotubes or exclusively within the nanorings. These combined observations indicate that the nature of the intermolecular organization and packing within the nanostructures significantly impacts the excited state properties of the materials.

In conclusion, we have demonstrated the hierarchical self-assembly of an n-type nanotube. The nanotube assembles via a monolayer nanoring that further stacks into the nanotube structure. The exceptional homogeneity in the structure and conformation of the constituent molecules leads to rapid energy migration within the nanotubes. The efficacy of these nanostructures as components of light-harvesting devices is currently under investigation.

Received: June 4, 2010
Published online: September 6, 2010

Keywords: amino acids · bolaamphiphiles · nanotubes · self-assembly · semiconductors

[1] B. J. Schwartz, *Annu. Rev. Phys. Chem.* **2003**, *54*, 141.
[2] a) D. T. McQuade, J. Kim, T. M. Swager, *J. Am. Chem. Soc.* **2000**, *122*, 5885; b) H. Sirringhaus, P. J. Brown, R. H. Friend, M. M. Nielsen, K. Bechgaard, B. M. W. Langeveld-Voss, A. J. H. Spiering, R. A. J. Janssen, E. W. Meijer, P. Herwig, D. M. de Leeuw, *Nature* **1999**, *401*, 685.
[3] a) L. Zang, Y. Che, J. S. Moore, *Acc. Chem. Res.* **2008**, *41*, 1596; b) A. C. Grimsdale, K. Mullen, *Angew. Chem.* **2005**, *117*, 5732; *Angew. Chem. Int. Ed.* **2005**, *44*, 5592; c) F. J. M. Hoeben, P. Jonkheijm, E. W. Meijer, A. P. H. J. Schenning, *Chem. Rev.* **2005**, *105*, 1491.
[4] *Carbon Nanotubes: Advanced Topics in the Synthesis Structure, Properties and Applications* (Eds.: A. Jorio, G. Dresselhaus, M. S. Dresselhaus), Springer, Berlin, **2008**.
[5] T. Yamamoto, T. Fukushima, T. Aida, *Adv. Polym. Sci.* **2008**, *220*, 1.
[6] a) J. P. Hill, W. S. Jin, A. Kosaka, T. Fukushima, H. Ichihara, T. Shimomura, K. Ito, T. Hashizume, N. Ishii, T. Aida, *Science* **2004**, *304*, 1481; b) Z. C. Wang, C. J. Medforth, J. A. Shelnutt, *J. Am. Chem. Soc.* **2004**, *126*, 16720; c) W. S. Horne, N. Ashkenasy, M. R. Ghadiri, *Chem. Eur. J.* **2005**, *11*, 1137; d) J. A. A. W. Elemans, R. Van Hameren, R. J. M. Nolte, A. E. Rowan, *Adv. Mater.* **2006**, *18*, 1251; e) A. Ajayaghosh, R. Varghese, S. Mahesh, V. K. Praveen, *Angew. Chem.* **2006**, *118*, 7893; *Angew. Chem. Int. Ed.* **2006**, *45*, 7729; f) W. Y. Yang, E. Lee, M. Lee, *J. Am. Chem. Soc.* **2006**, *128*, 3484; g) C. J. Medforth, Z. C. Wang, K. E. Martin, Y. J. Song, J. L. Jacobsen, J. A. Shelnutt, *Chem. Commun.* **2009**, 7261; h) P. P. Yao, H. F. Wang, P. L. Chen, X. W. Zhan, X. Kuang, D. B. Zhu, M. H. Liu, *Langmuir* **2009**, *25*, 6633.
[7] Bolaamphiphiles are amphiphilic molecules that contain hydrophilic groups on both ends of a hydrophobic skeleton. See Ref. [11].
[8] a) E.-K. Schillinger, E. Mena-Osteritz, J. Hentschel, H. G. Boerner, P. Baeuerle, *Adv. Mater.* **2009**, *21*, 1562; b) E. Jahnke, J. Weiss, S. Neuhaus, T. N. Hoheisel, H. Frauenrath, *Chem. Eur. J.* **2009**, *15*, 388; c) M. van den Heuvel, D. W. P. M. Lowik, J. C. M. van Hest, *Biomacromolecules* **2008**, *9*, 2727; d) S. R. Diegelmann, J. M. Gorham, J. D. Tovar, *J. Am. Chem. Soc.* **2008**, *130*, 13840; e) J. D. Tovar, B. M. Rabatic, S. I. Stupp, *Small* **2007**, *3*, 2024; f) E. Jahnke, A.-S. Millerioux, N. Severin, J. P. Rabe, H. Frauenrath, *Macromol. Biosci.* **2007**, *7*, 136; g) E. Jahnke, I. Lieberwirth, N. Severin, J. P. Rabe, H. Frauenrath, *Angew. Chem.* **2006**, *118*, 5510; *Angew. Chem. Int. Ed.* **2006**, *45*, 5383.
[9] a) H. Shao, T. Nguyen, N. C. Romano, D. A. Modarelli, J. R. Parquette, *J. Am. Chem. Soc.* **2009**, *131*, 16374; b) h. Shao, J. R. Parquette, *Chem. Commun.* **2010**, *46*, 4285.
[10] a) M. Sofos, D. A. Stone, D. K. Goswami, J. S. Okasinski, H. Jin, M. J. Bedzyk, S. I. Stupp, *J. Phys. Chem. C* **2008**, *112*, 2881; b) B. Song, H. Wei, Z. Q. Wang, X. Zhang, M. Smet, W. Dehaen, *Adv. Mater.* **2007**, *19*, 416.
[11] a) A. H. Fuhrhop, T. Y. Wang, *Chem. Rev.* **2004**, *104*, 2901; b) A. Meister, A. Blume, *Curr. Opin. Colloid Interface Sci.* **2007**, *12*, 138.
[12] For a recent example of an amino acid based bolaamphiphile, see: S. C. Yin, C. Wang, B. Song, S. L. Chen, Z. Q. Wang, *Langmuir* **2009**, *25*, 8968.
[13] a) M. Reches, E. Gazit, *Science* **2003**, *300*, 625; b) S. Matsumura, S. Uemura, H. Mihara, *Mol. BioSyst.* **2005**, *1*, 146; c) H. Shao, J. R. Parquette, *Angew. Chem.* **2009**, *121*, 2563; *Angew. Chem. Int. Ed.* **2009**, *48*, 2525.
[14] Y. Yan, A. de Keizer, A. A. Martens, C. L. P. Oliveira, J. S. Pedersen, F. A. de Wolf, M. Drechsler, M. A. C. Stuart, N. A. M. Besseling, *Langmuir* **2009**, *25*, 12899.
[15] a) A. P. H. J. Schenning, P. Jonkheijm, E. Peeters, E. W. Meijer, *J. Am. Chem. Soc.* **2001**, *123*, 409; b) F. Würthner, *Chem. Commun.* **2004**, 1564.
[16] J. Gawronski, M. Brzostowska, K. Kacprzak, H. Kolbon, P. Skowronek, *Chirality* **2000**, *12*, 263.
[17] M. Tomasulo, D. M. Naistat, A. J. P. White, D. J. Williams, F. M. Raymo, *Tetrahedron Lett.* **2005**, *46*, 5695.
[18] C. L. Zhan, P. Gao, M. H. Liu, *Chem. Commun.* **2005**, 462.
[19] a) J. V. Selinger, M. S. Spector, J. M. Schnur, *J. Phys. Chem. B* **2001**, *105*, 7157; b) M. S. Spector, K. R. K. Easwaran, G. Jyothi, J. V. Selinger, A. Singh, J. M. Schnur, *Proc. Natl. Acad. Sci. USA* **1996**, *93*, 12943.
[20] A. Shioi, T. A. Hatton, *Langmuir* **2002**, *18*, 7341.
[21] S. Vauthey, S. Santoso, H. Y. Gong, N. Watson, S. G. Zhang, *Proc. Natl. Acad. Sci. USA* **2002**, *99*, 5355.
[22] K. Takegoshi, S. Nakamura, T. Terao, *Chem. Phys. Lett.* **2001**, *344*, 631.
[23] C. P. Jaroniec, C. Filip, R. G. Griffin, *J. Am. Chem. Soc.* **2002**, *124*, 10728.
[24] a) C. Wasmer, A. Lange, H. Van Melckebeke, A. B. Siemer, R. Riek, B. H. Meier, *Science* **2008**, *319*, 1523; b) A. Lange, Z. Gattin, H. Van Melckebeke, C. Wasmer, A. Soragni, W. F. van Gunsteren, B. H. Meier, *ChemBioChem* **2009**, *10*, 1657; c) J. J. Helmus, K. Surewicz, P. S. Nadaud, W. K. Surewicz, C. P. Jaroniec, *Proc. Natl. Acad. Sci. USA* **2008**, *105*, 6284; d) J. J. Helmus, K. Surewicz, W. K. Surewicz, C. P. Jaroniec, *J. Am. Chem. Soc.* **2010**, *132*, 2393.
[25] Y. Posokhov, S. Alp, B. Koez, Y. Dilgin, S. Icli, *Turk. J. Chem.* **2004**, *28*, 415.

